IOSR Journal of Mechanical and Civil Engineering (IOSR-JMCE)
e-ISSN: 2278-1684,p-ISSN: 2320-334X, Volume 20, Issue 5 Ser. III (Sept. – Oct. 2023), PP 46-53
www.iosrjournals.org

The effect of Retrofitting RC beams with GFRP sheets under blast loads

Mahmoud Samak[1], Ehab Lotfy[2], Manar A. Ahmed[2], Erfan Abdel Latif[2]
[1]*(Civil Engineering, El-Arish High Institute for Engineering and Technology, North Sinai, Egypt)*
[2]*(Civil Engineering, Faculty of Civil Engineering/ Suez Canal University, Ismailia, Egypt)*

Abstract:
The blast load is the dynamic load that an engineer may face during the design procedure. This paper used the ABAQUS program to simulate reinforced concrete (RC)beams retrofitted with GFRP sheets subjected to blast loads. The experiment data is simulated in the ABAQUS program to validate the ABAQUS modeling, it was collected from a last experiment research. The deflection, reaction force, and damage mode of RC beams under blast loading are studied. The dimension models are 2500x 250 x 150 mm. The characteristic compressive strength of concrete (fcu) is 25 MPa. The parametric studies of ABAQUS models are the standoff distance (D), TNT weights, and retrofitting techniques of GFRP sheets. The results show that, RC beams are damaged in flexure-shear and flexure. the spallation area significantly affects scaled distance. The retrofitting techniques with GFRP sheets decrease the deflection and reaction force addition to enhance the resistance of beams to damage. It was observed that the G retrofitting technique significant effect than the GS and GSL retrofitting techniques.
Key Word*: Blast load, Explosion waves, RC beams, ABAQUS, GFRP, retrofitting techniques.*

Date of Submission: 18-10-2023 Date of Acceptance: 28-10-2023

I. Introduction

Several concrete buildings may be subjected to blast loads due to natural phenomena or human interventions. After World War, people began to identify the significance of keeping buildings from blast influence which was a specific challenge to design. Now this field has become one of the most substantial when designing buildings to withstand blast loads in numerous countries of the world. An explosion wave can technically be known as a rapid dissipation of energy which leads to a rapid increase in pressure. This pressure increases creating a wave called a “Blast Wave”. The amplitude pressure has two areas: the positive area and the negative area as shown in fig. 1. Where "ΔP" is the overpressure, which is the change between "Po" the ambient pressure, and "Ps" the maximum pressure, "t" is the time [1]–[5].

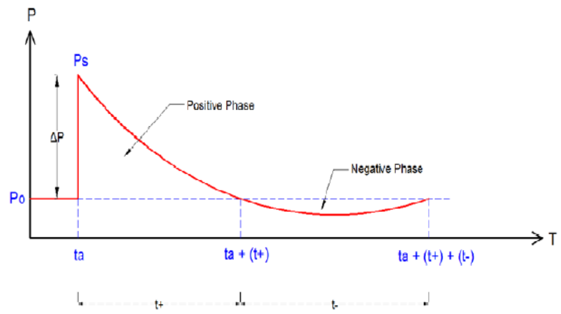

Figure 1: Ideal blast wave behavior.

Hopkinson-Cranz Scaling says that if any two bombs have equal scaled distances, they will give the same overpressure even if it has different weight and standoff distance[5]. Z is the scaled distance ($m/Kg^{1/3}$), D is the distance between the bomb and the building(meter), and W is the TNT weight (Kg).

$$Z = \frac{D}{\sqrt[3]{W}} \quad (1)$$

The explosion wave is represented on the RC as shown in Fig. 2. Once the blast wave achieves the beam, it can produce local compressive damages. With the spreading of wave within the beam and achieving the bottom face, it reflects and produces the tensile damage and the concrete spall damage at the beam bottom surface as shown in Fig. 2a. The localized damages, RC beams relation to their shear and flexural resistances could signify various flexural, shear, or flexure-shear failures exposed to several power and period of explosion wave. RC beams could undergo a flexural response when the explosion period is bigger than the natural vibration period of the beam as shown in fig.2b. In this class of failure mode, the beam may undergo the explosion energy, concrete strength, and reinforcement strength. Conversely, RC beams exposed to explosion waves for a very short period could undergo diagonal or direct shear failures as shown in fig. 2c is affected by the boundary conditions and detonation power. Additionally, between the flexural and shear failures, flexural-shear failure is achievable as shown in fig. 2d, when the beam is exposed to a medium range of detonation power and period [6].

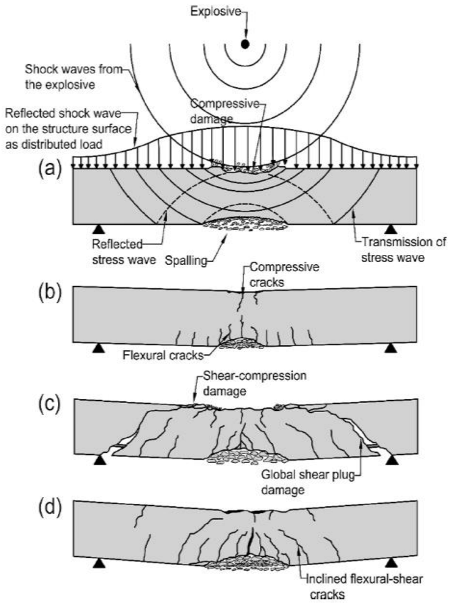

Figure 2: The failure mode of RC beams subjected to blast load: (a) local responses; (b) flexural failure; (c) shear failure; (d) flexural-shear failure.

II. Aim And Objectives

The research aim is to simulate the behavior of an RC beam under an explosion wave using ABAQUS. The objectives are to:

1) Show the response of the RC beam exposed to the blast waves.
2) Study the failure mode of the RC beam under blast waves.
3) Comparison between the retrofitting techniques of GFRP sheets.

III. Numerical Analysis

The finite element modeling is used to study the effect of factors on the behavior of RC beams under explosion waves by the ABAQUS program. The last experimental research validates with ABAQUS models.

Verification of the nonlinear finite element modeling

The experimental study was presented on RC beams under blast loading[7]. The dimensions of the beam were 1100 x 100 x 100 mm table 2. The reinforcement steel for all specimens was 6 mm. The stirrups spacing was 60 mm. The compressive strength of concrete was 40.45 MPa. The yield and ultimate strength of reinforcement steel were 395 and 501 MPa respectively.

Table 1: Experimental program.

Model	**Dimension (mm)**	**TNT mass (kg)**	**Standoff distance (m)**	**Scale distance (m/kg$^{1/3}$)**
B2-1	100x100x1100	0.36	0.4	0.57
B2-4		0.75	0.4	0.40

The experimental study was presented on RC beams under blast loading[8]. The dimensions of the beam were 220 x 300 x 2000 mm. The reinforcements of all these beams are with a diameter of 12 mm. The stirrups spacing was C8@80 mm and C8@ 150 mm. For a steel bar, the yield strength and the elastic modulus were 458 MPa and 193 GPa respectively. The concrete material grade was C40. The beam was simply supported with 100 mm hanging over at each edge. The TNT was over in the mid-span of the beam table 3.

Table 2: Blast protocol of concrete beams.

Model	Dimension (mm)	TNT mass (kg)	Standoff distance (m)	Scale distance (m/kg$^{1/3}$)
S12-1-2	220x300x2000	1	0.50	0.5000
S12-2		2	0.65	0.5159
S12-3		3	0.65	0.4507

RC beams and beam-columns transversely wrapped with SRP tested under blast load[9]. Ten RC members were tested under change blast load. The dimensions were 150 x 150 x 2100 mm as follows in table 4. The longitudinal and tied reinforcement were with diameter 6mm. The spacing of stirrups were 60mm. The compressive strength of concrete was 39.1 MPa. The yield and ultimate reinforcement strength were 500 MPa and 600 MPa respectively.

Table 3: Blast protocol of concrete beams.

Model	Dimension (mm)	C4 mass (kg)	TNT mass (kg)	Standoff distance (m)	Scale distance (m/kg$^{1/3}$)
B1	150x150x2100	20	25.8	2	0.677
C1		15	19.35	2	0.745

The models were adjusted until an agreeable error was obtained. The numerical search was prepared on RC beams subjected to explosion waves using the ABAQUS program. The validation was comparing mid-span deflection. Table 5 shows the comparison of mid-span displacements between experimental and ABAQUS models. As shown the change between experimental and numerical analysis results is agreeable.

Table 4: Maximum deflection for experimental and finite element modeling analysis.

Ref.	Model	Max. deflection (mm)		Error (%)
		Experimental	ABAQUS	
[7]	B2-1	9	9.07	0.78
	B2-4	40	37.45	6.38
[8]	S12-1-2	3.31	3.12	8.76
	S12-2	4.89	5.06	9.29
	S12-3	11.14	11.06	0.72
[9]	B1	22	20.31	7.68
	C1	8	8.74	9.25

Nonlinear finite element modeling

This thesis studies the behavior of RC beams subjected to blast load using ABAQUS. Beams with dimensions of 150 x 250 x 2500 mm were used in the numerical analysis. The characteristic compressive strength of concrete fcu is 25 MPa. The diameter of longitudinal reinforcement and transverse reinforcement is 10 and 6 mm respectively. The spacing between stirrups is variable 100 mm. The blast loading used in the ABAQUS was placed over the center of the RC beam as shown in fig. 3. The yield and ultimate strength of the reinforcing steel 6 mm were 240 MPa and 350 MPa respectively, and the reinforcing steel 10 mm are 390 MPa and 560 MPa, respectively. The U shape of GFRP sheets is used to retrofit the RC beams. It is an E-Glass fabric of 0.168 mm fiber thickness, 2500 MPa fiber tensile strength, and the modulus of elasticity was 72000 MPa. The three techniques used to retrofit the beams (total, shear, and flexure-shear wrapped) as shown in fig. 4. Tested parameters of this research are as follows in table 6:

1) The TNT weights.
2) standoff distance D.
3) The retrofitting techniques with GFRP sheets.

Table 5: Parametric study of ABAQUS models.

Parametric study		Symbols	Values
Z (m/kg$^{1/3}$)	TNT (Kg)	T_1	1.5
		T_2	8
		T_3	15
	Standoff distance (mm)	D_1	400
		D_2	1500
		D_3	3000
Retrofitting techniques		G	Total
		GSL	Shear wrapped

	GS	Flexure-shear wrapped

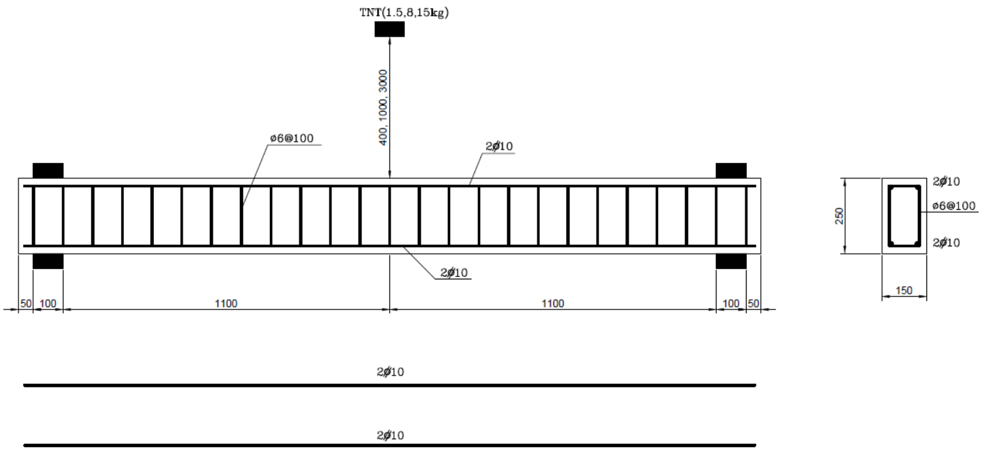

Figure 3: Details of ABAQUS models.

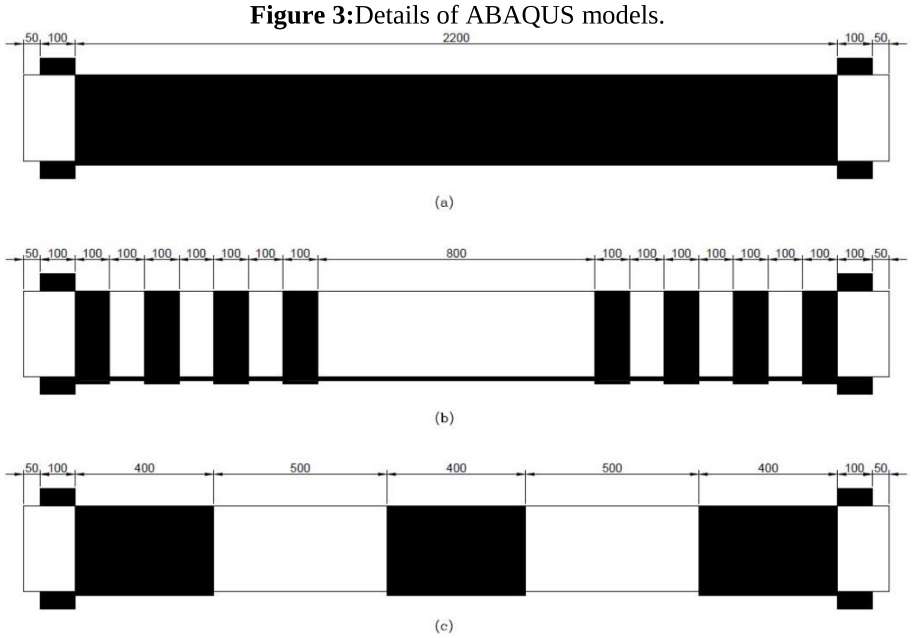

Figure 4: Details of retrofitting techniques (a) G, (b) GSL, and (c) GS.

The ABAQUS program is applied to analysis of RC beams. There are three main parts for modeling: the concrete body that is modeled using a solid element, steel reinforcement that is modeled as a rebar element, and FRP that is modeled as a shell element. The analysis step chosen was dynamic explicit. In finite elements, the concrete damage plasticity model (CDP) is used to model the behavior of concrete[2], [10]. For the reinforcing steel is considered as the elastic-plastic behavior. FRP was defined by using the elastic-plastic behavior with lamina type. The concrete and steel reinforcement geometry were modeled as solid deformable and wire deformable elements respectively. The concrete beam meshed as structural elements of 8 node hexahedral linear brick element (C3D8R) with a 20 mm mesh size while steel reinforcement was meshed with 2 node linear truss element (T3D2) with a 5 mm mesh size and FRP was meshed with 4 nodes doubly curved thin or thick shell element (S4R) with 20 mm mesh size. The constraint-embedded region option is modeled as an interaction between concrete and steel. The concrete is chosen as the host region and the steel reinforcement as the embedded region. The interaction between concrete and FRP is modeled using the constraint tie option, whereas the concrete and FRP are selected as the master surface and slave surface respectively. The blast load is described with Conventional Weapons Effects Program (CONWEP) interaction property. For the boundary condition, two ends of the beam are pinned.[11].

IV. Result

The simulations were run on thirty-six RC beams exposed to blast loading. The factors such as standoff distance, mass of TNT, and retrofitting technique of GFRP sheets have been studied. The deflection (Y), reaction forces (F), and damage mode against the last parameters are studied in this section.

Parametric study

Table 6: Maximum deflection, reaction force, and damage mode of control and retrofitting ABAQUS models.

Models	Y_{max} (mm)	$F_{max.}$ (KN)	Damage mode	Models	Y_{max} (mm)	$F_{max.}$ (KN)	Damage mode
T1D1	5.02	356.53	Spalling	T1D1G	1.33	75.55	Spalling
T1D2	1.43	206.76	Cracks	T1D2G	0.24	37.49	Cracks
T1D3	0.29	54.99	Intact	T1D3G	0.07	6.63	Intact
T2D1	143.76	272.26	Damage	T2D1G	8.37	167.83	Damage
T2D2	10.38	436.78	Spalling	T2D2G	1.12	133.89	Spalling
T2D3	1.62	190.57	Cracks	T2D3G	0.24	37.83	Intact
T3D1	436.69	253.42	Damage	T3D1G	18	213	Damage
T3D2	33.4	186.76	Damage	T3D2G	2.15	226.55	Spalling
T3D3	2.85	302.14	Cracks	T3D3G	0.41	73.14	Intact
T1D1GSL	9.49	48.27	Damage	T1D1GS	1.42	160.67	Spalling
T1D2GSL	0.51	43.89	Cracks	T1D2GS	0.37	66.62	Cracks
T1D3GSL	0.09	7.97	Intact	T1D3GS	0.1	20.91	Intact
T2D1GSL	47.06	162.18	Damage	T2D1GS	12.84	294.61	Damage
T2D2GSL	10.6	95.37	Damage	T2D2GS	1.8	219.78	Spalling
T2D3GSL	0.31	53	Intact	T2D3GS	0.38	84.01	Intact
T3D1GSL	92.81	202.42	Damage	T3D1GS	47.39	298.94	Damage
T3D2GSL	18.82	140.49	Damage	T3D2GS	5.55	278.38	Spalling
T3D3GSL	0.58	78.79	Cracks	T3D3GS	0.66	112.52	Cracks

Table 8 shows that there is almost no effect of the blast waves on the beam with the scaled distance of 2.62 m/kg1/3 .The maximum deflection was 0.45 mm. Many cracks occurred at the center portion and near upper supports with the scaled distance range of 0.87: 1.5 m/kg1/3. The maximum deflection range was 1.8: 3 mm. A part of the concrete at the top central beam is broken in addition to diagonal and flexural cracks developing from the lower edge and many cracks occurred near upper supports with scaled distance range 0.35: 0.5 m/kg1/3. The maximum deflection range is 6: 40 mm respectively. The core concrete of the center portion completely failed with the scaled distance range of 0.16: 0.2 m/kg1/3. The maximum deflection range was 164: 450 mm. The displacement and intensity of the failure region increased with the decrease in the scaled distance.

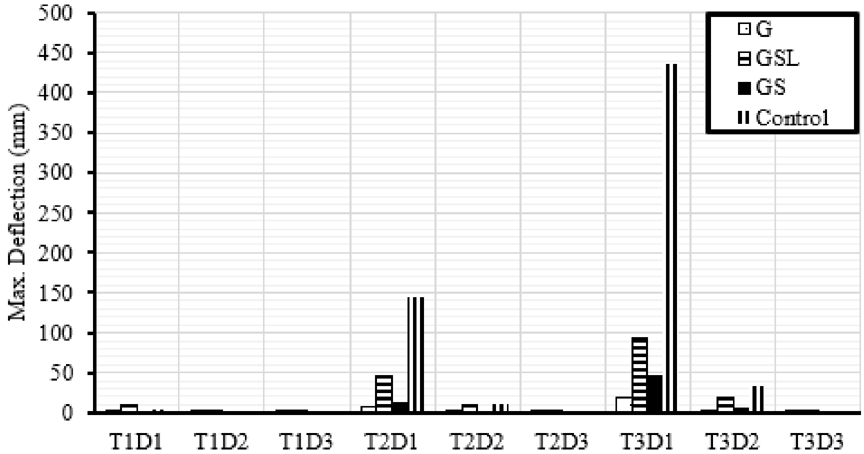

Figure 5: Max. deflection of retrofitted models with different techniques of GFRP sheets.

In fig. 5, retrofitting techniques with GFRP sheets, the deflection decreases with G than GS and GSL retrofitting techniques do not exceed 10, 12%, and 15% respectively. While with an increase in the TNT weight, the deflection increase does exceed 800%. Additionally, with an increase in the standoff distance, the deflection decreases with a ratio not less than 94 %. From the last results, the effect of G is better than GS and GSL retrofitting techniques on deflection. While it shows a significant effect of the scaled distance on deflection.

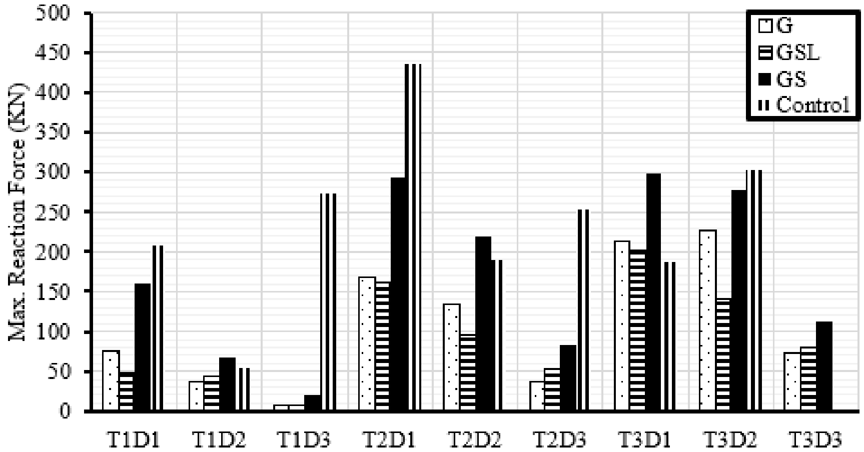

Figure 6: Max. the reaction force of retrofitted models with different techniques of GFRP sheets.

In fig. 6, retrofitting techniques with GFRP sheets, the reaction force decreases with G than GSL and GS retrofitting techniques do not exceed 10, 12%, and 15% respectively. while with an increase in the TNT weight, the reaction force increase does exceed 800% but with an increase in the standoff distance, the reaction force decreases with a ratio doesn't less than 94 %. From the last results, the effect of G is better than GSL and GS retrofitting techniques on reaction force. While it shows a significant effect of the scaled distance on reaction force.

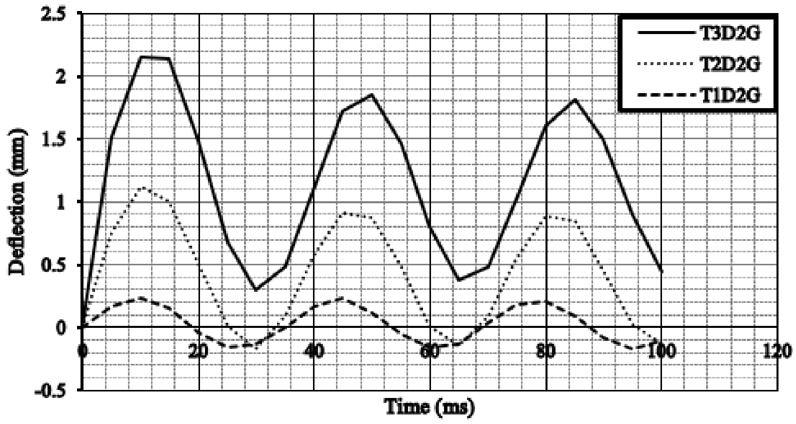

Figure 7: Deflection-time curve for D2G models with different TNT weights.

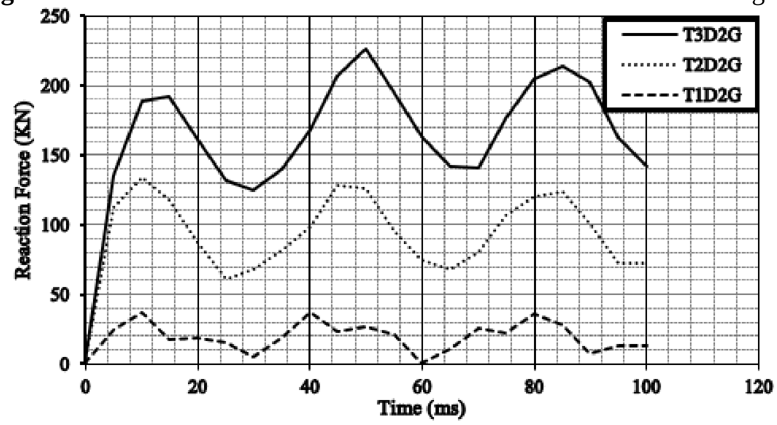

Figure 8: Reaction force-time curve for D2G models with different TNT weights.

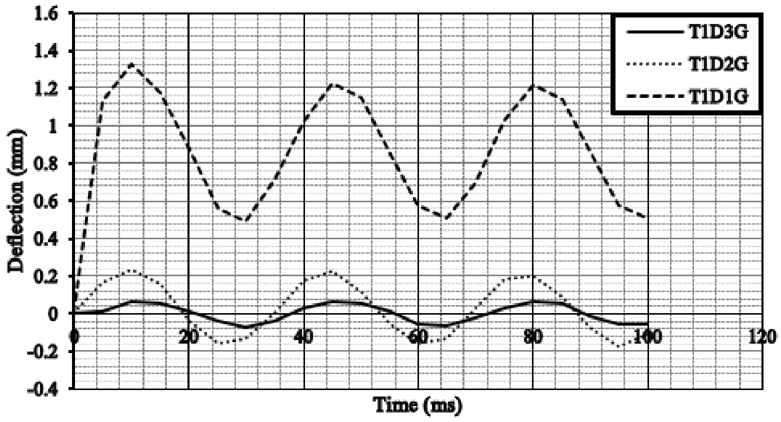

Figure 9: Deflection-time curve for T1G models with different standoff distances.

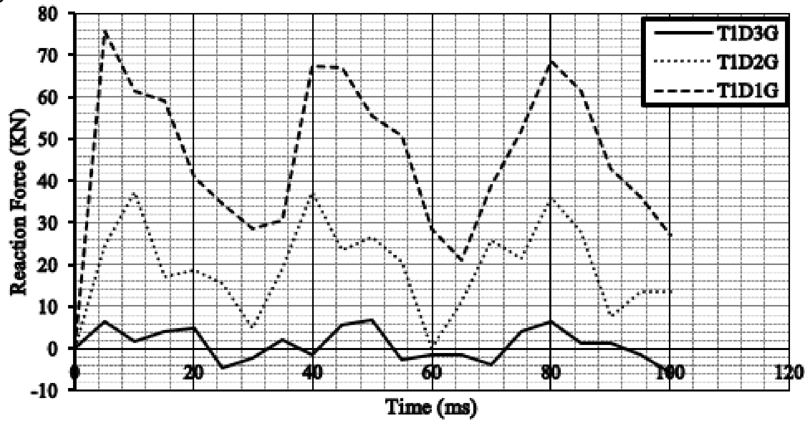

Figure 10: Reaction force-time curve for T1G models with different standoff distances.

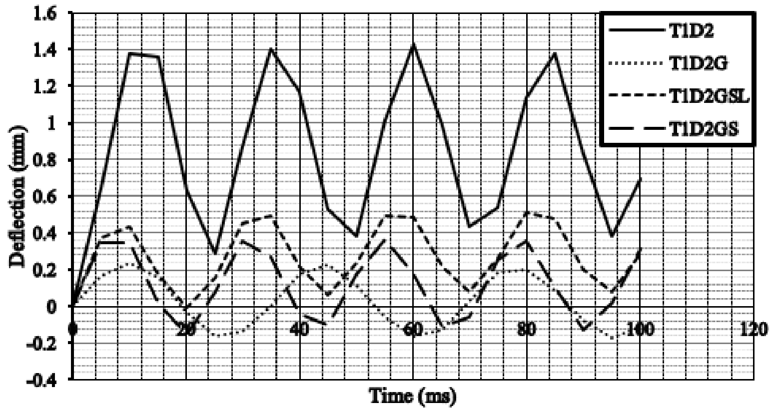

Figure 11: Deflection-time curve for T1D2 models with different retrofitting techniques.

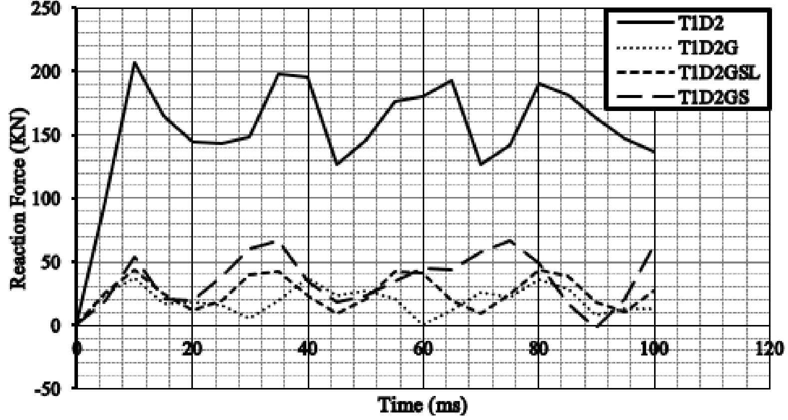

Figure 12: Reaction force-time curve for T1D2 models with different retrofitting techniques.

V. Discussion

From fig. 5 and 6, the effect of G is better than GS and GSL retrofitting techniques on reaction force and deflection. However, the scaled distance is agreed to be selected to be with blast event classification (close-in, intermediate, and far).

In fig. 7 and 8, illustrates the behavior of most models with an increase in the TNT weight, the reaction force, and deflection significantly increase. In fig. 9 and 10, illustrates the behavior of most models with an increase in the standoff distance, the reaction force, and deflection significantly decrease. Fig. 11 and 12, illustrate the behavior of all retrofitting models with FRP sheets, the reaction force and deflection significantly decrease with G, GS, and GSL techniques. Additionally, G techniques can resist the explosive shock than GSL and GS techniques, which are illustrated by streamlining the curves.

VI. Conclusion

This study proposed an ABAQUS model to study the behavior of RC beams subjected to explosion waves under parameters of TNT weights, standoff distance, and retrofitting technique. The numerical modeling results are compared with the previous research. The numerical results show the deflection, reaction force, and damage mode for RC beams. The conclusions are:

1. The finite element ABAQUS program agrees to predict the behavior of RC beams subjected to blast loads.
2. For different of Z, lower scaled distance is more signification than high scaled distance in deflection and reaction forces.
3. The use of GFRP sheets significantly decreases both deflection and the reaction force than the control models and enhances the damage mode as well.
4. It is noticed that the G technique is more ductile than the GS and GSL techniques, so the deflection and the reaction force are decreased with the G technique than with the GS and GSL techniques.
5. For retrofitting techniques, the G technique can resist explosive shock more than GSL and GS techniques, which are illustrated by streamlining the curves.

References

[1]. Y. Temsah, A. Jahami, J. Khatib, and M. Sonebi, "Numerical analysis of a reinforced concrete beam under blast loading," MATEC Web Conf., vol. 149, p. 02063, 2018, doi: 10.1051/matecconf/201814902063.
[2]. A. Jahami, Y. Temsah, and J. Khatib, "The efficiency of using CFRP as a strengthening technique for reinforced concrete beams subjected to blast loading," Int. J. Adv. Struct. Eng., vol. 11, no. 4, pp. 411–420, Dec. 2019, doi: 10.1007/s40091-019-00242-w.
[3]. Housing and Building National Research Center, Egyptian specification for blast resistant buildings SPEC 905. Cairo, 2016.
[4]. American Concrete Institute (ACI) 370r-14, Report for the design of concrete structures for blast effects. 2014.
[5]. Unified Facilities Criteria (UFC) 3-340-02, structures to resist the effects of accidental explosions. U.S. Department of Defense (DoD), 2008. [Online]. Available: http://dod.wbdg.org/.
[6]. C. Zhang, G. Gholipour, and A. A. Mousavi, "Nonlinear dynamic behavior of simply-supported RC beams subjected to combined impact-blast loading," Eng. Struct., vol. 181, pp. 124–142, Feb. 2019, doi: 10.1016/j.engstruct.2018.12.014.
[7]. D. Zhang et al., "Experimental study on scaling of RC beams under close-in blast loading," Eng. Fail. Anal., vol. 33, pp. 497–504, Oct. 2013, doi: 10.1016/j.engfailanal.2013.06.020.
[8]. S. Liu et al., "Blast responses of concrete beams reinforced with GFRP bars: Experimental research and equivalent static analysis," Compos. Struct., vol. 226, Oct. 2019, doi: 10.1016/j.compstruct.2019.111271.
[9]. M. Carriere, P. J. Heffernan, R. G. Wight, and A. Braimah, "Behaviour of steel reinforced polymer (SRP) strengthened RC members under blast load," Can. J. Civ. Eng., vol. 36, no. 8, pp. 1356–1365, Aug. 2009, doi: 10.1139/L09-053.
[10]. S. V Chaudhari and M. A. Chakrabarti, "Modeling of concrete for nonlinear analysis Using Finite Element Code ABAQUS," 2012.
[11]. "Abaqus/CAE User's Manual Abaqus 6.17 Abaqus/CAE User's Manual."